1-1-2018

From the Cover: 7,8-Dihydroxyflavone Rescues Lead-Induced Impairment of Vesicular Release: A Novel Therapeutic Approach for Lead Intoxicated Children

Xiao-Lei Zhang
New York Medical College

Jennifer L. McGlothan

Omid Miry

Kirstie H. Stansfield

Meredith K. Loth

See next page for additional authors

Recommended Citation

Zhang, X., McGlothan, J., Miry, O., Stansfield, K., Loth, M., Stanton, P., & Guilarte, T. (2018). From the Cover: 7,8-Dihydroxyflavone Rescues Lead-Induced Impairment of Vesicular Release: A Novel Therapeutic Approach for Lead Intoxicated Children. *Toxicological Sciences, 161* (1), 186-195. https://doi.org/10.1093/toxsci/kfx210

7,8-Dihydroxyflavone Rescues Lead-Induced Impairment of Vesicular Release: A Novel Therapeutic Approach for Lead Intoxicated Children

Xiao-lei Zhang[1], Jennifer L. McGlothan[2], Omid Miry[1], Kirstie H. Stansfield[3], Meredith K. Loth[2,3], Patric K. Stanton[1], Tomás R. Guilarte[2*]

[1]Department of Cell Biology & Anatomy
New York Medical College
Valhalla, NY

[2]Department of Environmental & Occupational Health
Robert Stempel College of Public Health & Social Work
Florida International University
Miami, FL

[3]Department of Environmental Health Sciences
Mailman School of Public Health
Columbia University
New York, NY

[*]Correspondence to:
Tomás R. Guilarte, Ph.D.
Dean, Robert Stempel College of Public Health & Social Work
Dept. Environmental & Occupational Health; Cognitive Neuroscience & Imaging
Florida International University
Miami, FL 33199
Phone: 305-348-5344
E-mail: tguilart@fiu.edu

ABSTRACT

Lead (Pb^{2+}) exposure during brain development inhibits neurotransmitter release resulting in impaired synapse formation, synaptic plasticity and learning. In primary hippocampal neurons in culture and hippocampal slices, Pb^{2+} exposure inhibits vesicular release and reduces the number of fast-releasing sites, an effect associated with Pb^{2+} inhibition of NMDA receptor-mediated trans-synaptic BDNF signaling. We hypothesized that TrkB receptor activation, the cognate receptor for BDNF, would rescue Pb^{2+}-induced impairments of vesicular release. Rats were chronically exposed to Pb^{2+} prenatally and postnatally until 50 days of age. This Pb^{2+} exposure paradigm enhanced paired-pulse facilitation representative of reduced vesicular release probability. Reductions in Pb^{2+}-induced release probability were also measured by both mean-variance analysis and direct two-photon imaging of vesicular release from hippocampal slices. We also found a Pb^{2+} impairment of calcium influx in presynaptic terminals. Intraperitoneal injections of the TrkB agonist 7,8-dihydroxyflavone (5 mg/kg) for 14-15 days in Pb^{2+} rats starting at postnatal day 35, reversed all Pb^{2+}-induced impairments of presynaptic transmitter release at Schaffer collateral-CA1 synapses. These data indicate that *in vivo* pharmacological activation of TrkB receptors can reverse long-term effects of chronic Pb^{2+} exposure on presynaptic terminals, pointing to TrkB receptor activation by small molecules as a promising therapeutic intervention in Pb^{2+}-intoxicated children.

KEYWORDS

7,8-dihydroxyflavone; vesicular release; lead neurotoxicity

Childhood lead (Pb^{2+}) intoxication is a significant public health problem in the United States and globally[1,2]. Recent episodes of Pb^{2+} exposure in children in communities like Flint, Michigan demonstrate the pervasive nature of the problem[3]. The National Resources Defense Council (NRDC) reports that millions of Americans get drinking water from water systems that have Pb^{2+} violations and the problem could be much larger, because systems known to have violations do not show up in government databases that track such problems. Despite nearly a century of knowledge on the detrimental effects of Pb^{2+} in children's development, the widespread presence of this poison in the global environment continues to affect children in the most vulnerable and economically disadvantaged segments of the population.

Studies have consistently demonstrated that one of the most prominent effects of Pb^{2+} in children is decreased capacity to learn, with devastating effects on cognitive and intellectual development[4-8], and in-school performance[9,10]. Early life Pb^{2+} intoxication diminishes intellectual capacity of children with an immeasurable cost to society. Human studies have shown that Pb^{2+} exposure in early life is associated with longitudinal declines in cognitive function[11], loss of brain volume[12,13], and emergence of mental disorders such as major depression and schizophrenia[14,15].

Our laboratory has provided the first working model by which Pb^{2+} exposure during the period of synaptogenesis can affect synapse development and function, that accounts for both presynaptic and postsynaptic effects of Pb^{2+} on the synapse[16-18]. Using a Pb^{2+} exposure paradigm during the period of synaptogenesis in primary hippocampal neurons, we found that Pb^{2+} inhibition of postsynaptic NMDA receptors (NMDAR) impairs CREB-dependent transcription of activity-regulated genes such as brain-derived neurotrophic factor (BDNF), and alters the function of its cognate receptor TrkB and

downstream signaling and alters vesicle movement[16-18]. These studies also showed that Pb^{2+}-induced impairment of BDNF trans-synaptic retrograde signaling decreases the presynaptic vesicular proteins synaptophysin and synaptobrevin and inhibits vesicular release[16]. The addition of exogenous BDNF to Pb^{2+}-exposed hippocampal neurons normalized synaptophysin and synaptobrevin levels and reversed the impairment in vesicular release, providing the first evidence of the beneficial effects of BDNF on Pb^{2+}-induced synaptic dysfunction[16]. Consistent with these observations, electrophysiological and two-photon imaging studies at Schaffer collateral-CA1 synapses in *ex vivo* hippocampal slices from rats chronically exposed to Pb^{2+} during development, revealed a marked inhibition of hippocampal Schaffer-collateral-CA1 synaptic transmission by inhibiting vesicular release[19].

In the present study, we determined whether BDNF activation of its cognate receptor, TrkB, could rescue the Pb^{2+}-induced deficits in vesicular release observed in Pb^{2+} exposed animals *in vivo*. We used 7,8-dihydroxyflavone (7,8-DHF), a small, CNS permeant molecule from the flavonoid family that is a BDNF mimetic and activates TrkB receptors[20]. 7,8-DHF exhibits promising therapeutic efficacy in animal models of neurodegenerative diseases[20-22]. Based on our previous *in vitro* studies demonstrating a beneficial effect of BDNF on Pb^{2+}-induced inhibition of vesicular release, we hypothesized that 7,8-DHF could be useful to assess in our *in vivo* Pb^{2+} exposure paradigm. Here we demonstrate that 7,8-DHF can rescue the inhibition of hippocampal Schaffer-collateral-CA1 vesicular release resulting from developmental Pb^{2+} exposure.

RESULTS

Blood Pb^{2+} levels and body weight of rats:

The Pb^{2+} exposure paradigm did not produce any overt toxicity based on body weight gain. Body weights at postnatal day 50 (PN50) rats were: 264.4 ± 11.9 g (n=10) for control animals plus or minus 7,8-DHF and 231.9 ± 10.0 g (n=14) for Pb^{2+}-exposed animals plus or minus 7,8-DHF ($p>0.05$). Further, blood Pb^{2+} levels of littermates to animals used in this study at PN50 were: 0.6 ± 0.1 μg/dL (n=67) for control animals and 22.2 ± 0.9 μg/dL (n=47) for Pb^{2+}-exposed animals. This exposure level is environmentally relevant and previous studies using this animal model have shown deficits in synaptic plasticity[23], decreased adult neurogenesis[24], and impairments of spatial learning and contextual fear conditioning[23,25,26].

7,8-DHF reverses the increase in paired-pulse facilitation at Schaffer collateral-CA1 synapses produced by Pb^{2+} exposure: Neuronal short-term presynaptic plasticity is often assessed by delivering paired-pulse stimulation, that is, two stimuli to the same synaptic pathway in close succession[27,28]. One form of paired-pulse modulation, paired-pulse facilitation (PPF), is typically attributed to an increase of release probability (*Pr*) during the second stimulus, arising from prior accumulation of residual Ca^{2+} near active zones and/or lingering effects of Ca^{2+} on a Ca^{2+} sensor[28,29]. This residual Ca^{2+}, when present at terminals that *fail* to release on the first stimulus, will cause them to release and increase response amplitude from the second stimulus. Therefore, if initial *Pr* is reduced, as by manipulations such as reducing extracellular [Ca^{2+}], the magnitude of PPF (the ratio of second to first response amplitude) should increase[28,29].

In Figure 1A the black trace shows that PPF in CA1 pyramidal neurons was elicited by two Schaffer collateral stimuli applied 30 ms apart. The red trace (Figure 1A) shows the larger PPF typical of a CA1 pyramidal neuron in a slice from a Pb^{2+} rat (Pb^{2+}/VEH) while the blue trace illustrates rescue of PPF in a slice from a Pb^{2+} rat that also received 7,8-DHF (Pb^{2+}/7,8-DHF). Administration of 7,8-DHF to control animals (CON/7,8-DHF; grey trace) did not alter PPF. When paired-pulse stimuli were applied at intervals varying from 20-70 msec, PPF was significantly increased compared to slices from untreated control rats (One-way ANOVA ($F(2,29)=9.786$, $p=0.0006$). PPF at a paired-pulse interval of 30 ms was significantly increased in slices from Pb^{2+}-treated rats compared to slices from control rats (post-hoc Tukey's multiple comparison with Duncan's correction: $p=0.008$). Moreover, 7,8-DHF treatment of lead exposed rats significantly reduced PPF at this 30 ms interval, compared to rats exposed to lead alone (post-hoc Tukey's multiple comparison with Duncan's correction: $p=0.029$), or to control rats (post-hoc Tukey's multiple comparison with Duncan's correction: $p=0.963$), as showed in Figure 1C. One-way ANOVA with repeated measures demonstrated a statistically significant increase in PPF at all inter-pulse intervals (Figure 1B red circles; $p=0.0064$) in lead treated rats compared to controls, while 7,8-DHF administration completely rescued PPF across the entire paired-pulse profile (Figure 1B, blue circles).

7,8-DHF reverses the impairment in vesicular release from the rapidly-recycling vesicle pool produced by Pb^{2+} exposure: To directly determine whether presynaptic vesicular release is altered by *in vivo* Pb^{2+} exposure, we used two-photon excitation to visualize release of the styryl dye FM1-43 from the rapidly-recycling pool (RRP) of presynaptic vesicles after selective loading by hypertonic shock in Schaffer collateral-CA1 terminals in hippocampal slices. Presynaptic vesicles in the RRP were first stimulated by a brief hypertonic shock to fuse with the membrane and release their

transmitter, which induces them to take up FM1-43 from the extracellular space, followed by endocytosis and recycling back into the rapidly-recycling pool for the next evoked release. We have used this method previously to show that generation of long-term potentiation (LTP) and long-term depression (LTD) is associated with persistent increases[30] or decreases[31] in the rate of stimulus-evoked FM1-43 de-staining at Schaffer collateral terminals, and that chronic early life Pb^{2+} exposure persistently reduces vesicular release from the RRP[19].

Figure 2 illustrates the effect of Pb^{2+} exposure on vesicular release from Schaffer collateral presynaptic terminals. Figure 2A shows representative pseudocolor images of FM1-43 labelled Schaffer collateral terminals before (Baseline) and after 12 minutes of 2 Hz stimulation in control slices from rats that received daily injections of vehicle (CON/VEH) or 7,8-DHF (CON/7,8-DHF), versus slices from Pb^{2+} rats with vehicle (Pb^{2+}/VEH) or Pb^{2+} rats that received 7,8-DHF (Pb^{2+}/7,8-DHF). The slice from the Pb^{2+}-exposed rat showed markedly slower stimulus-evoked de-staining compared to the control slice, while rapid de-staining was restored in the slice from the Pb^{2+} rat that received 7,8-DHF. Figure 2B summarizes the time courses of all slices, showing the markedly slower vesicular release evoked by 2 Hz stimulation of Schaffer collateral terminals in field CA1 of slices from Pb^{2+} rats (red filled circles) compared to controls treated with vehicle (black open circles) or controls treated with 7,8-DHF (grey solid circles), and the rescue of this effect in slices from Pb^{2+} rats treated with 7,8-DHF (blue solid circles). Statistics with one way ANOVA ($F(3,102)=50.73$, $p<0.0001$) on the initial time constant of release calculated from a single exponential fit of the first 6 times points[30,31] exhibited a significant slower decay constant in rats exposed to Pb^{2+} alone (red bar, $p=0.0001$), compared to control rats treated with vehicle (open bar), 7,8-DHF alone (grey bar, $p=0.504$), or Pb^{2+}-exposed rats also given 7,8-DHF (blue bar, $p=0.711$).

7,8-DHF reverses Pb^{2+}-induced reductions in presynaptic Schaffer collateral release probability measured by variance-mean analysis: Variance-mean (VM) analysis using a binomial model of synaptic transmission has been employed to study neurotransmitter release probability at a variety of synapses[32,33]. It is typically applied to steady-state sequences of single evoked EPSCs recorded while varying extracellular [Ca^{2+}], or delivering long repetitive trains of stimulation of different frequencies, each resulting in a range of mean response size with variance that is a parabolic function of *Pr*[34-37]. In this method, low extracellular [Ca^{2+}] yields low *Pr*, release failures and low EPSC variance, high extracellular [Ca^{2+}] yields high *Pr*, few failures and, again, low EPSC variance, and physiological extracellular [Ca^{2+}] yields intermediate *Pr* and higher EPSC variance. We have applied this method to directly estimate presynaptic *Pr* at Schaffer collateral-CA1 synapses, comparing normal slices to slices from Pb^{2+}-exposed rats using the identical protocol as in the current study[19].

Figure 3A demonstrates that the VM relationship obtained by varying extracellular [Ca^{2+}] was parabolic, with maximum variance at the peak of the parabola. In pyramidal hippocampal neurons from Pb^{2+} rats (Pb^{2+}/VEH), individual slice data point (Figure 3A, red circles) and mean amplitudes (Figure 3B, red circles) at different [Ca^{2+}], converted to *Pr*, were reduced along the same parabolic fit at all three [Ca^{2+}], consistent with a reduction in presynaptic release probability compared to CON/VEH/7,8-DHF (black open circles). It should be noted that the CON/VEH/7,8-DHF is the combined data from CON/VEH and CON/7,8-DHF animals since there was no significant differences between these two groups. The groups were combined in order to make panel A and B graphs easier to understand. The actual data for each group is provided in Table 1.

Across all experiments (Table 1), *Pr* calculated by this method was significantly reduced in slices from Pb^{2+}/VEH rats at low (1/4 mM, p=0.007), medium (2/2 mM, p=0.005) and high (4/1 mM, p=0.005) $[Ca^{2+}]/[Mg^{2+}]$ ratios (One-way ANOVA with repeated measures ($F(8,69)=25.14$, p=0.001). Figure 4 shows a variance/mean versus mean linear plot, where the line fit from pyramidal neurons from a CON/VEH (black dotted line) versus a Pb^{2+}/VEH (red dotted line) rat significantly differed in slope (p=0.015), consistent with a presynaptic site of reduced *Pr*. This shift in slope was rescued in a slice from a Pb^{2+} rat treated with 7,8-DHF (Figure 4, blue dotted line). Again, the CON/7,8-DHF data was not different from CON/VEH and it was not included to simplify the graph, but it is provided in Table 2. These shifts in *Pr* were not associated with significant changes in number of release sites (N) or quantal size (Q) across all slices (Table 2).

7,8-DHF reverses Pb^{2+}-induced reductions in presynaptic calcium influx into Schaffer collateral terminals: Calcium channels (P/Q and N-type) are the major source of action potential mediated Ca^{2+} influx into presynaptic terminals. Previous studies have shown that Pb^{2+} inhibits calcium channels in cultured cells, an effect that is reversible by washing the cellular preparation[38]. If Pb^{2+} exposure chronically alters the activity of these channels, this could indirectly contribute to alterations in *Pr*. To directly test whether chronic Pb^{2+} exposure produces a persistent inhibition of presynaptic Ca^{2+} influx, and to determine if 7,8-DHF can reverse such effects, we injected Mg^{2+} Green-AM, a calcium indicator dye that is membrane-permeable[39], directly into stratum radiatum of field CA1 of hippocampal slices. Mg^{2+} Green positive fluorescent puncta were visualized in field CA1 using two-photon excitation. Figure 5 demonstrates the kinetics of Mg^{2+} Green fluorescence increases in response to a 100 Hz burst of four Schaffer collateral stimuli. We have shown previously that these responses persist in the presence of NMDA and AMPA receptor antagonists, despite the loss of fEPSPs, are blocked by cadmium and

omega conotoxin, and co-localize with FM4-64, confirming a presynaptic nature for these calcium transients[40].

Comparison of mean fluorescence increases of representative stimulus-evoked presynaptic Ca^{2+} influx transients in Schaffer collateral terminals in slices from vehicle control (CON/VEH; Figure 5A black trace) or control treated with 7,8-DHF (CON/7,8-DHF; Figure 5A grey trace), versus Pb^{2+} rats (Pb^{2+}/VEH; Figure 5A red trace) and Pb^{2+} rats treated with 7,8-DHF (Pb^{2+}/7,8-DHF; Figure 5A, blue trace), revealed that action potential-dependent Ca^{2+} influx was reduced in amplitude by Pb^{2+} exposure, and that 7,8-DHF was able to reverse this reduction in presynaptic Ca^{2+} influx. Figure 5B summarizes these results across all slices, showing that Schaffer collateral presynaptic terminals in hippocampal slices from Pb^{2+} rats (red bar) exhibited reduced Ca^{2+} influx (One-way ANOVA with repeated measures $F(3,28)=5.233$, $p=0.0054$) compared to vehicle control slices (black bar, $p=0.0129$), 7,8-DHF treated slices (grey bar, $p=0.0192$), or slices from rats exposed to Pb^{2+} plus 7,8-DHF injections (blue bar, $p=0.0269$). Taken together, our data indicate that chronic exposure to Pb^{2+} during development results in a persistent reduction in presynaptic *Pr* that may be due to both reduced Ca^{2+} influx, and actions downstream of presynaptic Ca^{2+} influx at the level of SNARE protein-mediated exocytosis[16-18]. Consistent with its effects in rescuing *Pr*, daily injection of 7,8-DHF was also able to rescue the effects of Pb^{2+} exposure in reducing presynaptic Ca^{2+} influx at Schaffer collateral terminals in the hippocampus.

DISCUSSION

Our current study identifies a novel therapeutic target with the potential to treat Pb^{2+}-intoxicated children. Daily postnatal administration of the cell permeant TrkB receptor agonist 7,8-DHF, which readily crosses the blood-brain barrier, completely rescued Pb^{2+}-induced reductions in vesicular release and presynaptic Ca^{2+} influx, supporting its potential as a novel treatment for the cognitive effects of early life Pb^{2+} exposure. 7,8-DHF is a naturally occurring small molecule in the flavonoid family of polyphenolic compounds found in *Godmania aesculifoloia, Tridax procumbens*, and primula tree leaves[41,42]. It has been shown to be neuroprotective in preclinical studies[43,44]. However, further studies are needed to determine whether the rescue of transmitter release by 7,8-DHF is long-lasting or permanent, and whether it rescues behavioral impairments associated with chronic developmental exposure to Pb^{2+}.

Previous studies using acute exposure to Pb^{2+} in cultured cells have shown inhibition of Ca^{2+} channels by Pb^{2+}, an effect that is reversed upon washout of Pb^{2+} from the cells[38]. There could be additional mechanisms by which Pb^{2+} persistently alters vesicular release, such as changes in levels of SNARE proteins that we have shown previously[16,17]. In this study, fluorescent imaging of presynaptic Ca^{2+} influx showed that Pb^{2+} exposure was associated with reductions in voltage-dependent Ca^{2+} channel-mediated Ca^{2+} entry that were completely reversed by 7,8-DHF. Previously, we found that presynaptic Ca^{2+} fluorescent signals evoked by brief 20 Hz bursts of stimulation showed only a small, early reduction in amplitude of presynaptic Ca^{2+} signals in slices from Pb^{2+} rats[19], leading us to use higher frequency 100 Hz bursts of stimulation in this study. Our present findings suggest that developmental Pb^{2+} exposure can persistently impair presynaptic Ca^{2+} entry, and have additional downstream effects at the level of vesicular SNARE protein-mediated docking, recycling, and long-term stability of the

release complex, consistent with our previous findings in hippocampal neuronal cultures[16], and hippocampal slices from Pb^{2+} rats[19].

In this study, rats were exposed to Pb^{2+} chronically during gestation, postnatally and continuing through to young adulthood. The artificial cerebrospinal fluid used to maintain slice viability during experiments did not contain Pb^{2+}, indicating that the effects observed were the result of the *in vivo* Pb^{2+} exposure. Our studies have previously shown[16] that BDNF synthesis and release are decreased in cultured hippocampal neurons exposed to Pb^{2+}, and are associated with reductions in levels of SNARE proteins and inhibition of vesicular release. These effects of *in vitro* Pb^{2+} exposure, were rescued by exogenous BDNF, consistent with our present findings. Stansfield et al.[18], using the same Pb^{2+} exposure paradigm in cultured neurons, showed that Pb^{2+} may impair the transport of BDNF-containing vesicles, possibly by altering Huntingtin phosphorylation at a site promoting anterograde BDNF vesicle movement. This effect of Pb^{2+} resulted in impaired BDNF release, decreasing TrkB activation, and phosphorylation of synapsin I. Our current findings further support the hypothesis that BDNF receptor agonists and treatments such as enriched environments that increase BDNF levels and release[45,46], may be able to rescue the effects of chronic Pb^{2+} exposure we observed in more intact hippocampal synaptic networks. Further, previous studies from our laboratory have shown that environmental enrichment can reverse Pb^{2+}-induced impairments of spatial learning in rats of similar age and Pb^{2+} treatment[47]. This study also showed that Pb^{2+}-exposed rats placed in an enriched environment that reverses learning deficits, also exhibit increased BDNF gene expression in the hippocampus[47], supporting our current data implicating the BDNF-TrkB system in Pb^{2+} neurotoxicity and suggesting the BDNF mimetic 7,8-DHF as a potential therapy for Pb^{2+}-intoxicated children.

METHODS

Chemicals: Chemicals for extra- and intracellular solutions were purchased from Sigma-Aldrich (St. Louis, MO). Neurotransmitter receptor antagonists were purchased from Tocris Cookson (Minneapolis, MN), and FM1-43 from Invitrogen (Grand Island, NY).

Blood Pb^{2+} analysis: Blood Pb^{2+} levels in samples from littermates were measured using the LeadCare system (Magellan Diagnostics, N. Billerica, MA).

Animals: Adult female Long-Evans rats (250 g) were purchased from Charles River, Inc. (Wilmington, MA) and randomly placed on diet containing 0 (control) or 1500 ppm lead acetate (PbAc) (Dyets, Bethlehem, PA) 10 days prior to breeding with non-exposed Long-Evans males (300 g). Litters were culled to 10 pups on postnatal day 1 (PN1). Dams were maintained on their respective diet and at PN21 male pups were weaned onto the same diet and maintained until PN50. All rats are housed in plastic cages at 22 ± 2°C on a 12/12 light:dark cycle. Food and water were allowed ad libitum. Each litter is a single experimental unit for statistical purposes, so that for each experiment only one animal per litter was used for one data point. All studies were conducted in accordance with the United States Public Health Service's Policy on Human Care and Use of Laboratory Animals under protocols approved by Institutional Animal Care and Use Committees from each university.

Hippocampal slice electrophysiology: Experiments were conducted as described previously[19,30,31]. At 50 ± 2 days of age, rats were deeply anesthetized with isoflurane, decapitated and their brains rapidly removed and submerged in ice-cold artificial cerebrospinal fluid (ACSF, 2–4 °C), containing (in mM): 124 NaCl, 4 KCl, 2 $MgCl_2$, 2

$CaCl_2$, 1.25 NaH_2PO_4, 26 NaHCO3, 10 glucose; at pH 7.4, gassed continuously with 95% O_2/5% CO_2). Brains were hemisected, the frontal lobes cut off, and individual hemispheres glued using cyanoacrylate adhesive onto a stage immersed in ice-cold ACSF gassed continuously with 95% O_2/5% CO_2 during slicing. We cut 400 µm thick coronal slices using a vibratome (Leica VT1200S), and transferred them to an interface holding chamber for incubation at room temperature for a minimum of 1 hr before transferring to a submerged recording chamber continuously on a Zeiss Axioskop microscope continuously perfused at 3 ml/min with oxygenated ACSF at 32 ± 0.5 °C.

Whole cell patch-clamp recordings were performed in CA1 pyramidal neurons using standard techniques. Patch pipettes (R=3-4 MΩ) were filled with recording solution containing (in mM): 135 $CsMeSO_3$, 8 NaCl, 10 HEPES, 2 Mg-ATP, 0.3 Na-GTP, 0.5 EGTA, and 1 QX-314 (275 mOsm, pH 7.25 adjusted with $Cs(OH)_2$). Access resistance was carefully monitored, and only cells with stable access resistance (<5% change) were included in analyses. CA1 pyramidal cells were recorded under voltage clamp using a MultiClamp 700B (Axon Instruments) with Clampex (v9). Recording signals were filtered through an eight-pole Bessel low-pass filter with a 3 kHz cutoff frequency, digitized at 10 kHz, and sampled using Clampex (v9). Neurons were clamped at –60 mV, and Schaffer collateral-evoked EPSCs were delivered by a bipolar stimulating electrode (FHC, USA, 50-100 pA, 100 µs duration). EPSC slopes were calculated by linear interpolation of the initial downward current from 20% to 80% of the maximum EPSC amplitude. Paired-pulse facilitation was assessed by applying a pair of Schaffer collateral stimuli at intervals of 10-125 msec, and the ratio of slopes of the second to the first response was calculated, so that numbers greater than 1.0 represented facilitation, less than 1.0 inhibition.

Two-photon laser scanning microscopy

Vesicular release FM1-43 fluorescence measurements: Fluorescence was visualized using a customized two-photon laser-scanning Olympus BX61WI microscope with a 60x/0.90W water immersion infrared objective lens and an Olympus multispectral confocal laser scan unit. The light source was a Mai-Tai™ laser (Solid-State Laser Co., Mountain View, CA), tuned to 860 nm for exciting Magnesium Green and 820 nm for exciting FM1-43. Epifluorescence was detected with photomultiplier tubes of the confocal laser scan head with pinhole maximally opened and emission spectral window optimized for signal over background. In the transfluorescent pathway, a 565 nm dichroic mirror was used to separate green and red fluorescence to eliminate transmitted or reflected excitation light (Chroma Technology, Rockingham, VT). After confirming the presence of Schaffer collateral-evoked fEPSPs >1 mV in amplitude in CA1 *stratum radiatum*, and inducing LTP, 10 μM 6-cyano-7-nitroquinoxaline-2,3-dione (CNQX) was bath-applied throughout the rest of the experiment to prevent synaptically-driven action potentials in CA3 pyramidal neurons from accelerating dye release. Presynaptic boutons were loaded by bath-applying 5 μM FM1-43 (Molecular Probes) in hypertonic ACSF supplemented with sucrose to 800 mOsm for 25 sec to selectively load the rapidly-recycling pool (RRP)[30,31], then returned to normal ACSF. Stimulus-induced destaining was measured after 30 min perfusion with dye-free ACSF, by bursts of 10 Hz bipolar stimuli (150 μs DC pulses) for 2 sec applied once each 30 sec. We fitted a single exponential to the first 6 fluorescence time course values, and decay time constants between groups compared by two-tailed Student's t-test, as we have shown previously that the early release reflects vesicular release from the RRP prior to recycling and reuse of vesicles[30,31].

388

389 *Presynaptic Ca^{2+} influx fluorescence measurements:* Using established methods for
390 measuring [Ca^{2+}] transients[48], we filled Schaffer collateral presynaptic fibres with
391 Magnesium Green AM. Briefly, an ejection electrode (tip diameter, 5-10 μm) containing
392 Magnesium Green AM (1 mM Magnesium Green AM, 10% DMSO, 1% pluronic acid in
393 ACSF) was lowered into the Schaffer collateral pathway between the stimulating
394 electrode and the presynaptic terminal field to be observed, air pressure pulses (6-9 psi,
395 100-200 msec) controlled by a Picospritzer (General Valve Corp. USA) were applied to
396 the electrode until a small bright spot (≈10 mm in diameter) was observed. Thirty
397 minutes elapsed to allow dye to sufficiently diffuse into presynaptic boutons prior to
398 commencing imaging. To verify that magnesium green selectively loaded presynaptic
399 terminals, FM4-64 was loaded with high [K^+]o at the end of the experiment. To measure
400 Ca^{2+} dynamics, stimulus-evoked fluorescence signals were collected by scanning at 200
401 Hz in surface-scanning mode (XYT). Baseline fluorescence (F_0) was averaged over four
402 images, and $\Delta F/F$ calculated as $(\Delta F/F)_{(t)}=(F_{(t)}-F_0)/F_0$.
403

404 *Estimation of presynaptic release probability by variance-mean (VM) analysis:* Variance-
405 mean (VM) analysis according to a binomial model of synaptic transmission is a method
406 that has been employed to study transmitter release at many synapses[32,33,49]. It is mainly
407 applied to steady-state sequences of evoked EPSCs recorded under a variety of
408 conditions by varying extracellular [Ca^{2+}], or delivering long repetitive trains of stimulation
409 of different frequencies, each resulting in a range of mean response size[34-37].
410

411 We used three ratios of [Ca^{2+}]/[Mg^{2+}] in ACSF (4/1, 2/2, and 1/4 mM) to alter release
412 probability at Schaffer collateral synapses. Experiments began by establishing stable
413 whole-cell recording from a CA1 pyramidal neuron, and then perfusing the slice with 4/1

414 $[Ca^{2+}]/[Mg^{2+}]$ ACSF. Cells were voltage-clamped at -65 mV, and 100 μs constant-current
415 stimulus pulses were delivered to Schaffer collateral/commissural fiber axons every 10
416 sec to evoke an EPSC. Stable recordings for 8-10 min were made in 4/1 $[Ca^{2+}]/[Mg^{2+}]$,
417 before replacing the perfusate with 1/4 mM $[Ca^{2+}]/[Mg^{2+}]$ ACSF. After EPSCs decreased
418 in amplitude and restabilized, which usually took 5-8 min, EPSCs were recorded for an
419 additional 8 min. Slices were then perfused with 2/2 mM $[Ca^{2+}]/[Mg^{2+}]$ ACSF. After EPSC
420 amplitudes had again stabilized, another 8 min of recordings were made. To induce
421 LTD, slices were exposed to either 10 μM NMDA or 25 μM DHPG in 2/2 mM
422 $[Ca^{2+}]/[Mg^{2+}]$ ACSF for three or five min, respectively, durations which reliably induced
423 LTD lasting hours. After drug exposure, slices were perfused with 2/2 mM $[Ca^{2+}]/[Mg^{2+}]$
424 ACSF for >30 min, to verify expression of LTD, and then the same sequence of
425 $[Ca^{2+}]/[Mg^{2+}]$ ACSF applications was repeated. To ensure that postsynaptic AMPA
426 receptors were responding to non-saturating glutamate concentration, a requirement for
427 VM analysis, experiments were performed in a low concentration of the AMPA receptor
428 antagonist 6,7-dinitroquinoxaline-2,3-dione (DNQX, 100 nM).
429
430 *7,8-DHF administration:*
431 7,8-Dihydroxyflavone hydrate (DHF, Sigma-Aldrich, St Louis, MO) was dissolved in
432 phosphate-buffered saline (PBS) containing 17% dimethylsulfoxide (DMSO). Male rats
433 received daily intraperitoneal injections of 5 mg/kg 7,8-DHF or 17% DMSO vehicle daily
434 for 14-15 consecutive days starting when they were 35-42 days of age. Rats were
435 sacrificed for slice preparation twenty-four hours after the last 7,8-DHF administration.
436
437 *Statistics:* Power analysis showed a group size of 6 animals per treatment group with
438 significance level pre-set to $p<0.05$ could detect between group differences of 10% for
439 vesicular transmitter release time constants and release probability at a power of 85%

with typical parameter standard deviations. Data sets did not deviate significantly from normal distribution (D'Agostino-Pearson omnibus normality test), and did not exhibit significant differences in parameter variances (F-test). Slices and treatments were randomized, with treated and control slices examined in parallel on the same or sequential days. While all analyses were automated, the investigator was not blinded to treatment group. Student's t-test was used to determine differences between the control and Pb^{2+} treated groups for each particular measure. In analyses requiring comparisons between multiple groups, a one-way ANOVA with Sidak's Multiple Comparisons analysis was used with post-hoc Tukey's test for individual group comparisons. Significance level was preset to $p < 0.05$.

Data Availability: Following calculation of EPSP slopes, paired-pulse ratios or optical time courses of vesicular release and presynaptic calcium influx, all data will be made available upon request. Image analysis was performed with ImageJ (NIH), statistical analyses with GraphPad Prism v6 (La Jolla, CA), and custom-built, proprietary software was used to control the multi-photon laser scanner for FM1-43 imaging experiments, which is copyrighted by the designer and cannot be made available.

ACKNOWLEDGEMENTS: This work was supported by grants ES006189 and ES020465 from the National Institute of Environmental Health Sciences to TRG.

AUTHOR CONTRIBUTIONS:

X.Z.: experimental planning, analysis and execution; writing and editing of manuscript. J.L.M.: experimental planning and execution; writing and editing of manuscript. O.M.: experimental execution; K.H.S.: experimental execution; M.K.L.: experimental execution; P.K.S.: experimental planning, analysis, and direction; writing and editing of manuscript; T.R.G.: conceptualized overall studies and received funding, experimental planning and direction of study; writing and editing of manuscript.

COMPETING INTERESTS:

The authors declare no competing financial interests.

REFERENCES

1. Tong, S., von Schirnding, Y.E. & Prapamontol, T. Environmental lead exposure: a public health problem of global dimensions. *Bull. World Hlth. Org.* 78, 1068-1077 (2000).
2. Toscano, C.D. & Guilarte, T.R. Lead Neurotoxicity: From Exposure to Molecular Effects. *Brain Res. Rev.* 49, 529-554 (2005).
3. Hanna-Atisha, M., LaChance, J., Sadler, R.C. & Champney Schnepp, A. Elevated blood lead levels in children associated with the Flint drinking water crisis: A spatial analysis of risk and public health response. *Am. J. Public Health* 106, 283-290 (2016).
4. Bellinger, D.C., Stiles, K.M. & Needleman, H.L. Low level lead exposure, intelligence and academic achievement: a long term follow up. *Pediatrics* 90, 855-861 (1992).
5. Canfield, R.L., Henderson, C.R. Jr., Cory-Slechta, D.A., Cox, C., Jusko, T.A. & Lanphear, B.P. Intellectual impairment in children with blood lead concentrations below 10 ug per deciliter. *N. Engl. J. Med.* 348, 1517-1526 (2003).
6. Lanphear, B.P., Hornung, R., Khoury, J., Yolton, K., Baghurst, P., Bellinger, D.C., Canfield, R.L., Dietrich, K.N., Bornschein, R., Greene, T., Rothenberg, S.J., Needleman, H.L., Schnaas, L., Wasserman, G., Graziano, J. & Roberts, R. Low-level environmental lead exposure and children's intellectual function: An international pooled analysis. *Environ. Health Perspect.* 113, 894-899 (2005).
7. Jusko, T.A., Henderson, C.R., Lanphear, B.P., Cory-Slechta, D.A., Parsons, P.J. & Canfield, R.L. Blood lead concentrations < 10 ug/dl and child intelligence at 6 years of age. *Environ. Health Perspect.* 116, 243-248 (2008).
8. Schwartz, B.S., Stewart, W.F., Bolla, K.I., Simon, P.D., Bandeen-Roche, K., Gordon, P.B., Links, J.M. & Todd, A.C. Past adult lead exposure is associated with longitudinal decline in cognitive function. *Neurology* 55, 1144-1150 (2000).

9. Magzamen, S., Imm, P., Amato, M.S., Havlena, J.A., Anderson, H.A., Moore, C.F. & Kanarek, M.S. Moderate lead exposure and elementary school end-of-grade examination performance. *Ann. Epidemiol.* 23, 700-707 (2013).
10. Evens, A., Hryhorczuk, D., Lanphear, B.P., Rankin, K.M., Lewis, D.A., Forst, L. & Rosenberg, D. The impact of low-level lead toxicity on school performance among children in the Chicago Public Schools: a population-based retrospective cohort study. *Environ. Health* 14, 21 (2015).
11. Stewart, W.F., Schwartz, B.S., Davatzikos, C., Shen, D., Liu, D., Wu, X., Todd, A.C., Shi, W., Bassett, S. & Youssem, D. Past adult lead exposure is linked to neurodegeneration measured by brain MRI. *Neurology* 66, 1476-1484 (2006).
12. Cecil, K.M., Brubaker, C.J., Adler, C.M., Dietrich, K.N., Altaye, M., Egelhoff, J.C., Wessel, S., Elangovan, I., Hornung, R., Jarvis, K. & Lanphear, B.P. Decreased brain volume in adults with childhood lead exposure. *PLoS Med.* 5, e112 (2008).
13. Rizzoli, S.O. & Betz, W.J. Synaptic vesicle pools. *Nat. Rev. Neurosci.* 6, 57-69 (2005).
14. Bouchard, M.F., Bellinger, D.C, Weuve, J., Matthews-Bellinger, J., Gilman, S.E., Wright, R.O., Schwartz, J. & Weisskopf, M.G. Blood lead levels and major depressive disorder, panic disorder, and generalized anxiety disorder in US young adults. *Arch. Gen. Psychiatry* 66, 1313-1319 (2009).
15. Guilarte, T.R., Opler, M. & Pletnikov, M. Is lead exposure in early life an environmental risk factor for schizophrenia? Neurobiological connections and testable hypotheses. *Neurotoxicology* 33, 560-574 (2012).
16. Neal, A.P., Stansfield, K.H., Worley, P.F., Thompson, R.E. & Guilarte, T.R. Lead exposure during synaptogenesis alters vesicular release proteins and impairs vesicular release: potential role of NMDA receptor-dependent BDNF signaling. *Toxicol. Sci.* 116, 249-263 (2010).

536 17. Neal, A.P. & Guilarte, T.R. Molecular Neurobiology of Pb^{2+}: effects on synaptic
537 function. *Mol. Neurobiol.* 42, 151-160 (2010).
538 18. Stansfield, K.H., Pilsner, J.R., Lu, Q., Wright, R.O. & Guilarte, T.R. Dysregulation of
539 BDNF-TrkB signaling in developing hippocampal neurons by Pb^{2+}: implications for an
540 environmental basis of neurodevelopmental disorders. *Toxicol. Sci.* 127, 277-295
541 (2012).
542 19. Zhang, X.L., Guariglia, S.R., McGlothan, J.L., Stansfield, K.H., Stanton, P.K. &
543 Guilarte, T.R. Presynaptic mechanisms of lead neurotoxicity: effects on vesicular
544 release, vesicle clustering and mitochondrial number. *PLoS ONE* 10, e0127461
545 (2015).
546 20. Liu, C., Chan, C.B. & Ye, K. 7,8-dihydroxyflavone, a small molecular TrkB agonist, is
547 useful for treating various BDNF-implicated human disorders. *Transl. Neurodegener.*
548 5, 2 (2016).
549 21. Devi, L. & Ohno, M. 7,8-dihyrdoxyflavone, a small-molecule TrkB agonist, reverses
550 memory deficits and BACE1 elevation in a mouse model of Alzheimer's disease.
551 *Neuropsychopharmacology* 37, 434-444 (2012).
552 22. Jiang, M., Peng, Q., Liu, X., Jin, J., Hou, Z., Zhang, J., Mori, S., Ross, C.A., Ye, K. &
553 Duan, W. Small-molecule TrkB receptor agonists improve motor function and extend
554 survival in a mouse model of Huntington's disease. *Hum. Mol. Genet.* 22, 2462-2470
555 (2013).
556 23. Nihei, M.K., Desmond, N.L., McGlothan, J.L., Kuhlmann, A.C. & Guilarte, T.R. N-
557 methyl-D-asparatate receptor subunit changes are associated with lead-induced
558 deficits of long-term potentiation and spatial learning. *Neuroscience* 99, 233-242
559 (2000).

24. Verina,.T., Rohde, C.A. & Guilarte, T.R. Environmental lead exposure during early life alters granule cell neurogenesis and morphology in the hippocampus of young adult rats. *Neuroscience* 145, 1037-1047 (2007).

25. Kuhlmann, A.C., McGlothan, J.L. & Guilarte, T.R. Developmental lead exposure causes spatial learning deficits in adult rats. *Neurosci. Lett.* 233, 101-104 (1997).

26. McGlothan, J.L., Karcz-Kubicha, M. & Guilarte, T.R. Developmental lead exposure impairs extinction of conditioned fear in young adult rats. *NeuroToxicology* 29, 1127-1130 (2008).

27. Andersen, P. & Lømo, T. Control of hippocampal output by afferent volley frequency. *Progress in Brain Research: Structure and Function of the Limbic System*, eds Tokizane, T. & Adey, R.W. (Elsevier Science), 400-412 (1967).

28. Zucker, R.S. Short-term plasticity. *Annu. Rev. Neurosci.* 12, 13-31 (1989).

29. Neher, E. Vesicle pools and Ca^{2+} microdomains: new tools for understanding their roles in neurotransmitter release. *Neuron* 20, 389-399 (1998).

30. Stanton, P.K., Winterer, J. & Müller, W. Imaging LTP of presynaptic release of FM1-43 from the rapidly-recycling vesicle pool at Schaffer collateral-CA1 synapses in rat hippocampal slices. *Eur. J. Neurosci.* 22, 2451-2461 (2005).

31. Stanton, P.K., Winterer, J., Bailey, C.P., Kyrozis, A., Raginov, I., Laube, G., Veh, R.W., Nguyen, C.Q. & Müller, W. Long-term depression of presynaptic release from the readily-releasable vesicle pool induced by NMDA receptor-dependent retrograde nitric oxide. *J. Neurosci.* 23, 5936-5944 (2003).

32. Clements, J.D. & Silver, R.A. Unveiling synaptic plasticity: a new graphical and analytical approach. *Trends Neurosci.* 23, 105-113 (2000).

33. Silver, R.A. Estimation of nonuniform quantal parameters with multiple-probability fluctuation analysis: theory, application and limitations. *J. Neurosci. Methods* 130, 127-141 (2003).

586 34. Silver, R.A., Momiyama, A. & Cull-Candy, S.G. Locus of frequency-dependent
587 depression identified with multiple-probability fluctuation analysis at rat climbing fibre-
588 Purkinje cell synapses. *J. Physiol.* 510, 881-902 (1998).
589 35. Reid, C.A. & Clements, J.D. Postsynaptic expression of long-term potentiation in the
590 rat dentate gyrus demonstrated by variance-mean analysis. *J. Physiol.* 518, 121-30
591 (1999).
592 36.Oleskevich, S., Clements, J. & Walmsley, B. Release probability modulates short-
593 term plasticity at a rat giant terminal. *J. Physiol.* 524, 513-523 (2000).

594 37. Foster, K.A. & Regehr, W.G. Variance-mean analysis in the presence of a rapid
595 antagonist indicates vesicle depletion underlies depression at the climbing fiber
596 synapse. *Neuron* 43, 119-131 (2004).
597 38. Peng, S., Hajela, R.K. & Atchison, W.D. Characteristics of block by Pb^{2+} of function
598 of human neuronal L-, N-, and R-type Ca^{2+} channels transiently expressed in human
599 embryonic kidney 293 cells. *Mol. Pharm.* 62, 1418-1430 (2002).
600 39. Brustein, E., Marandi, N., Kovalchuk, Y., Drapeau, P. & Konnerth, A. "In vivo"
601 monitoring of neuronal network activity in zebrafish by two-photon Ca^{2+} imaging.
602 *Pflugers Arch.* 446, 766-773 (2003).
603 40. Zhang, X.L., Upreti, C. & Stanton, P.K. Gβγ and the C-terminus of SNAP-25 are
604 necessary for long-term depression of transmitter release. *PLoS One* 6, e20500
605 (2011).
606 41. Taddei, A. & Rosas-Romero, A.J. Bioactivity studies of extracts from Tridax
607 procumbens. *Phytomedicine* 7, 235-238 (2000).
608 42. Bhutia, T.D. & Valant-Vetschera, K.M. Diversification of exudate flavonoid profiles in
609 further Primula spp. *Nat. Prod. Commun.* 7, 587-589 (2012).

610 43. Jang, S.W., Liu, X., Yepes, M., Shepherd, K.R., Miller, G.W., Liu, Y., Wilson, W.D.,
611 Xiao, G., Blanchi, B., Sun, Y.E. & Ye, K. A selective TrkB agonist with potent
612 neurotrophic activities by 7,8-dihydroxyflavone. *Proc. Natl. Acad. Sci. USA* 107,
613 2687-2692 (2010).
614 44. Zhang, Z., Liu, X., Schroeder, J.P., Chan, C.B., Song, M., Yu, S.P., Weinshenker, D.
615 & Ye, K. 7,8-dihydroxyflavone prevents synaptic loss and memory deficits in a
616 mouse model of Alzheimer's disease. *Neuropsychopharmacology* 39, 638-650
617 (2014).
618 45. Ickes, B.R., Pham, T.M., Sanders, L.A., Albeck, D.S., Mohammed, A.H. & Granholm,
619 A.C. Long-term environmental enrichment leads to regional increases in
620 neurotrophin levels in rat brain. *Exp. Neurol.* 164, 45-52 (2000).
621 46. Rossi, C., Angelucci, A., Costantin, L., Braschi, C., Mazzantini, M., Babbini, F.,
622 Fabbri, M.E., Tessarollo, L., Maffei, L., Berardi, N. & Caleo, M. Brain-derived
623 neurotrophic factor (BDNF) is required for the enhancement of hippocampal
624 neurogenesis following environmental enrichment. *Eur. J. Neurosci.* 24, 1850-1856
625 (2006).
626 47. Guilarte, T.R., Toscano, C.D., McGlothan, J.L. & Weaver, S.A. Environmental
627 enrichment reverses cognitive and molecular deficits induced by developmental lead
628 exposure. *Ann. Neurol.* 53, 50-56 (2003).
629 48. Regehr, W. & Tank, D. Selective fura-2 loading of presynaptic terminals and nerve
630 cell processes by local perfusion in mammalian brain slice. *J. Neurosci. Meth.* 37,
631 111-119 (1991).
632 49. Zhang, X.L., Zhou, Z.Y., Winterer, J., Müller, W. & Stanton, P.K. NMDA-dependent,
633 but not group I mGluR-dependent, LTD at Schaffer collateral-CA1 synapses is
634 associated with long-term reduction of release from the rapidly recycling presynaptic
635 vesicle pool. *J. Neurosci.* 26, 10270-10280 (2006).

FIGURES

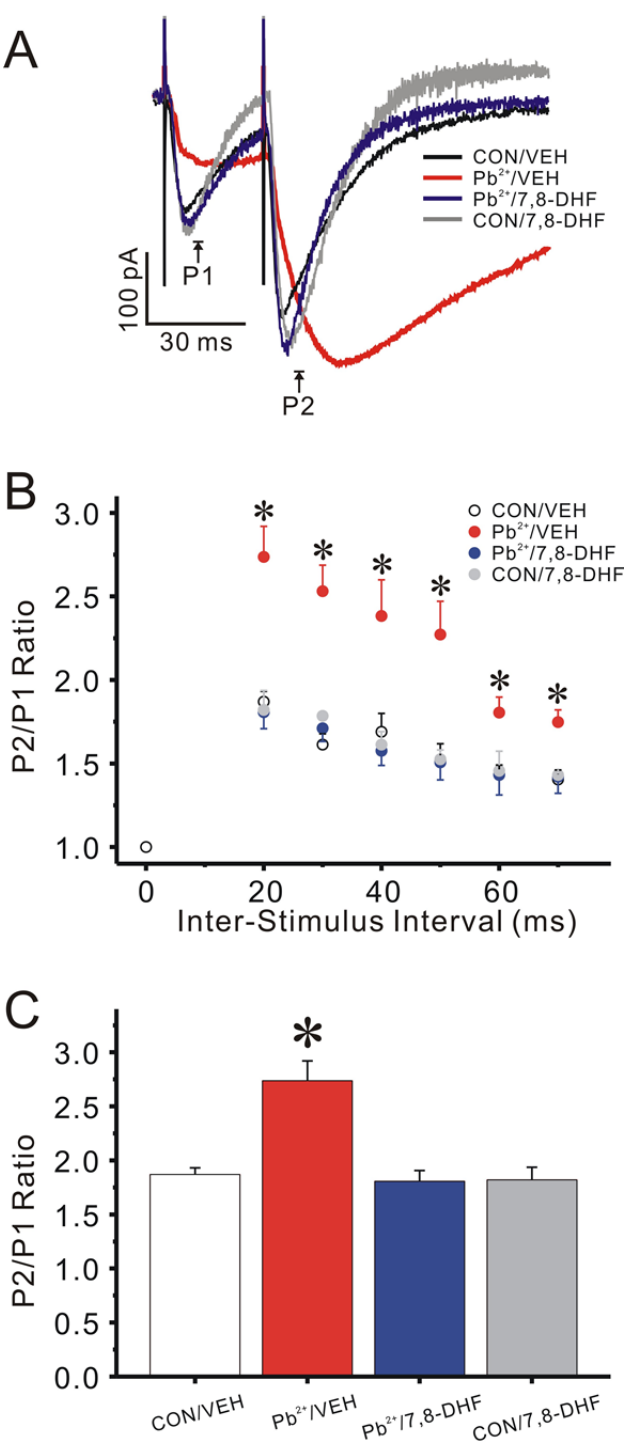

Figure 1: 7,8-DHF reverses the increase in paired-pulse facilitation (PPF) produced by Pb^{2+} exposure at Schaffer collateral-CA1 synapses in rat hippocampus. **(A)** Representative excitatory postsynaptic currents (EPSC) in field CA1 in response to Schaffer collateral paired-pulse stimuli at a 30 ms interstimulus interval (ISI) in slices from Control (CON/VEH; black trace), Pb^{2+}-treated (Pb^{2+}/VEH; red trace) and Pb^{2+} + 7,8-DHF-treated rats (Pb^{2+}/7,8-DHF; blue trace), illustrating the ability of 7,8-DHF to reverse Pb^{2+}-induced increases in PPF. **(B)** Mean ± SEM EPSC PPF P2/P1 ratio as a function of ISI, where PPF was significantly enhanced for ISI 20-70 ms in slices from Pb^{2+}-treated (filled red circles, N=9 slices) versus controls (open black circles, N=13 slices), and this effect was rescued by treatment of Pb^{2+} rats with 7,8-DHF (filled blue circles, N=10 slices) ($p<0.05$). **(C)** Mean ± SEM ratio

of P2/P1 (30 ms ISI) at Schaffer collateral-CA1 synapses in slices from control (open bar), Pb^{2+}-treated (red bar), and Pb^{2+} plus 7,8-DHF-treated rats (blue bar), showing that increased PPF in Pb^{2+}-treated rats ($p<0.05$) was rescued by 7,8-DHF co-administration.

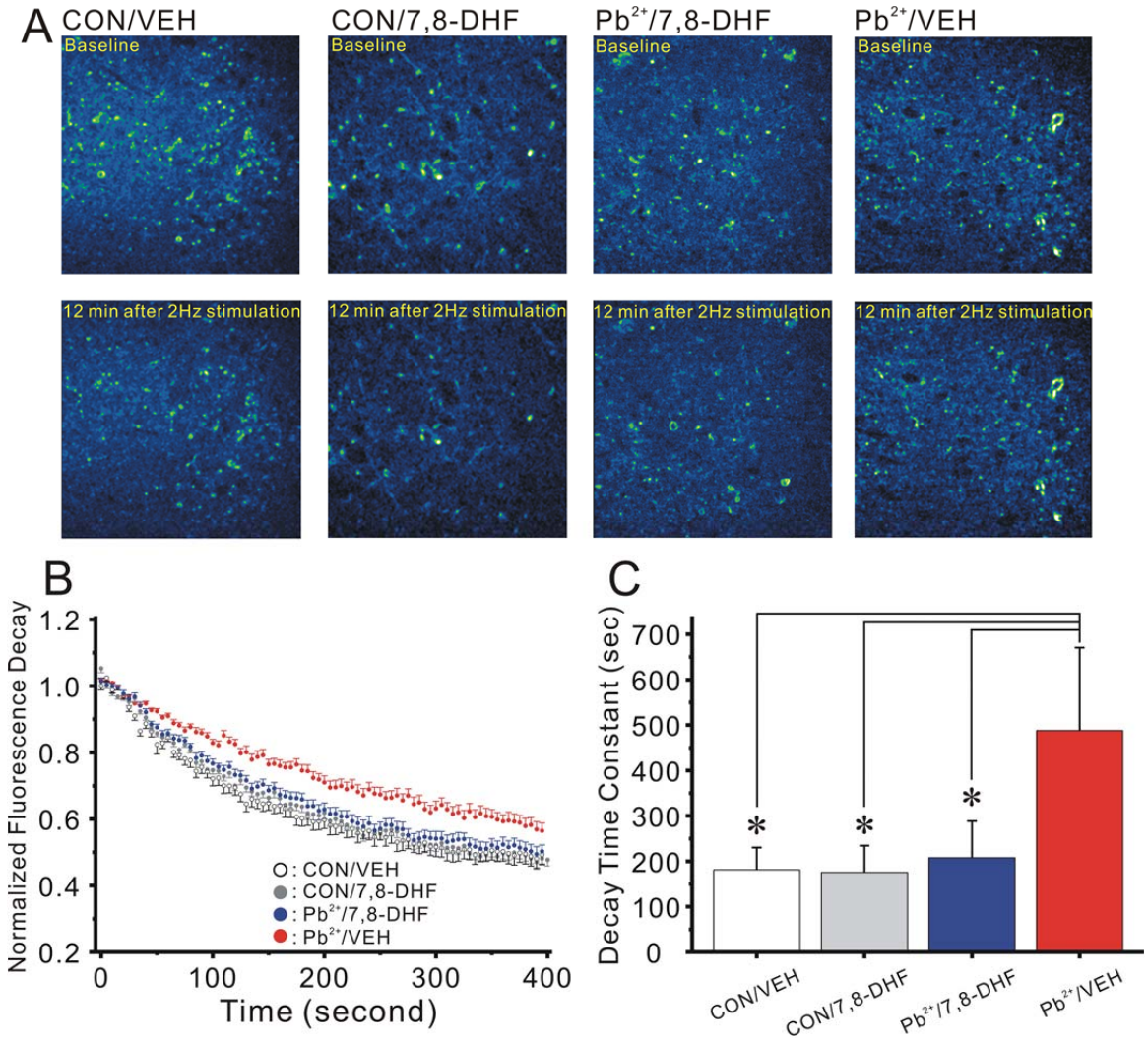

Figure 2: Two-photon laser scanning microscopic (TPLSM) images of FM1-43 vesicular release from Schaffer collateral terminals in field CA1 of hippocampal slices show that Pb^{2+}-induced persistent reduction in release probability is rescued by 7,8-DHF. **(A)** Representative TPLSM pseudocolor images of FM1-43 loaded presynaptic terminals in *stratum radiatum* of field CA1 in hippocampal slices from a Pb^{2+} rat (Pb^{2+}/VEH), versus a

rat treated with Pb^{2+} plus 7,8-DHF (Pb^{2+}/7,8-DHF), and one treated with DHF alone (CON/7,8-DHF), or control vehicle (CON/VEH) imaged prior to (Baseline) and after 12 min 2 Hz Schaffer collateral stimulation (Calibration Bar: 5 μm). **(B)** Time course (Mean ± SEM) of stimulus-evoked FM1-43 de-staining from puncta in field CA1 of hippocampal slices in response to 2 Hz Schaffer collateral stimulation in slices from control rats (open circles, N=8 slices, 35 puncta) versus Pb^{2+}-treated (red circles, N=6 slices, 30 puncta), and Pb^{2+} plus 7,8-DHF-treated rats (grey diamonds, N=8 slices, 36 puncta). **(C)** Mean ± SEM of initial fluorescence decay time constant in slices from Pb^{2+}-treated rats (Pb^{2+}/VEH), versus rats treated with Pb^{2+} plus 7,8-DHF (Pb^{2+}/7,8-DHF), and control rats treated with 7,8-DHF alone (CON/7,8-DHF) or vehicle (CON/VEH). All slices from Pb^{2+} rats showed significantly slower de-staining of Schaffer collateral terminals ($p<0.05$) compared to control slices, and this reduction was completely rescued by 7,8-DHF.

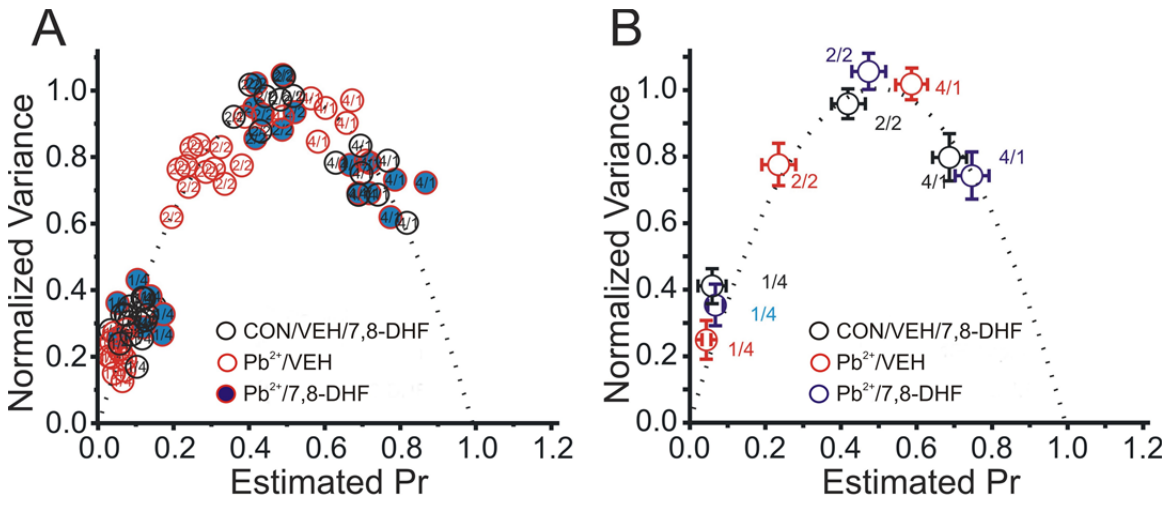

Figure 3: Chronic Pb^{2+} exposure is associated with reduced presynaptic vesicular release probability at Schaffer collateral-CA1 terminals assessed by variance/mean analysis. **(A)** Individual variance/mean data points, corrected to estimate P_r, at each

689 $[Ca^{2+}]_o$ for each CON/VEH/7,8-DHF (open black circles), each slice from a Pb^{2+} rat
690 (Pb^{2+}/VEH; open red circles), and each slice from a Pb^{2+} rat administered 7,8-DHF
691 (Pb^{2+}/7,8-DHF; blue circles). Data from all groups of slices were well fit by a single
692 parabola forced to pass through 0,0 with Pb^{2+} synapses shifted to the left, consistent
693 with a presynaptic reduction in P_r from chronic Pb^{2+} exposure. This shift was rescued by
694 7,8-DHF. **(B)** Mean ± SEM of variance/mean points in slices from CON/VEH/7,8-DHF
695 (black circles; N=11), Pb^{2+}/VEH (red circles; N=8), and Pb^{2+}/7,8-DHF (blue circles; N=8),
696 normalized to the maximal peak amplitude recorded at 4 mM $[Ca^{2+}]_o$.
697

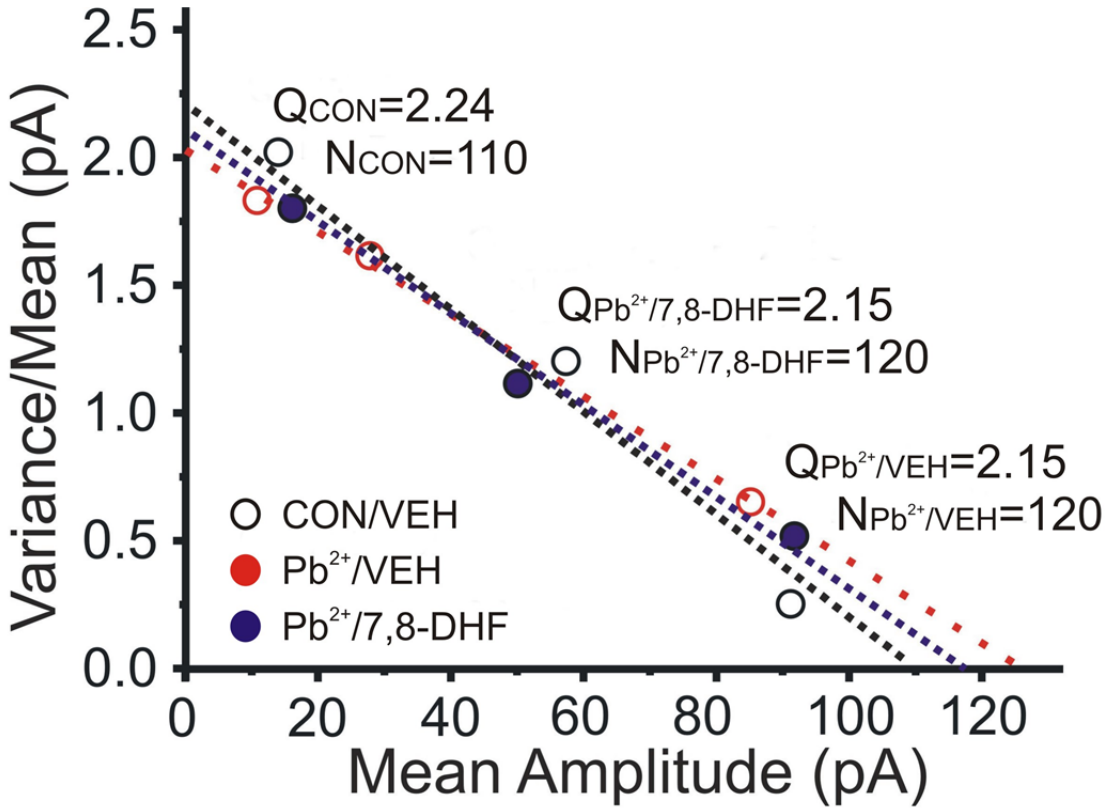

698

699 **Figure 4:** Plot of variance/mean ratio versus mean EPSC amplitude (pA) from a single
700 representative slice, which converts the parabolic relationship between mean and
701 variance to a linear one. The number of release sites (N) was derived by estimating the

slope of the linear fit, while the y-intercept denotes quantal size (Q) of the EPSC. The reduction in slope indicates that chronic Pb^{2+} exposure (Pb^{2+}/VEH; red dotted line) was associated with a reduction in presynaptic P_r compared to a control slice (CON/VEH; dotted black line), that was partially reversed in a slice from a Pb^{2+}-exposed rat administered 7,8-DHF (Pb^{2+}/7,8-DHF; dotted blue line).

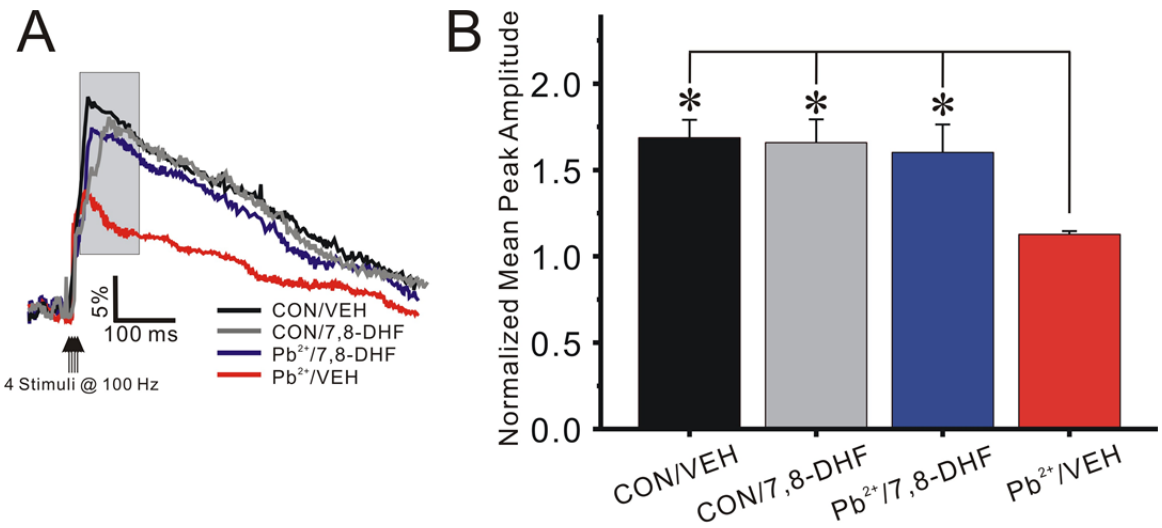

Figure 5: 7,8-DHF rescues Pb^{2+}-induced reductions in presynaptic Ca^{2+} influx into Schaffer collateral terminals. **(A)** Representative fluorescent transients evoked by Schaffer collateral stimulation in single presynaptic terminals of a Control slice (CON/VEH; black trace), a control slice with 7,8-DHF (CON/7,8-DHF; grey trace), a slice from a Pb^{2+} rat (Pb^{2+}/VEH; red trace), and a slice from a Pb^{2+} rat administered 7,8-DHF (Pb^{2+}/7,8-DHF; blue trace). **(B)** Mean ± SEM presynaptic stimulus-evoked Mg^{2+}-Green fluorescence increases in presynaptic terminals in response to a burst of Schaffer collateral stimuli (4x20Hz) in slices from control (CON/VEH, N=8 slices, 16 terminals) versus Pb^{2+}-exposed (Pb^{2+}/VEH, N=8 slices, 14 terminals) rats, and slices from Pb^{2+}-exposed rats co-administered 7,8-DHF (Pb^{2+}/7,8-DHF, N=8 slices, 16 terminals). Ca^{2+}

719 influx transients were significantly smaller in terminals of Pb^{2+}-exposed rat slices
720 compared to either controls or 7,8-DHF rescued slices ($p<0.05$).
721
722
723 **Table 1:** Presynaptic release probability estimated from variance/mean analysis as a
724 function of ratio of $[Ca^{2+}]/[Mg^{2+}]$

Ca^{2+}/Mg^{2+}	CON/VEH		CON/7,8-DHF		Pb^{2+}/VEH		Pb^{2+}/7,8-DHF	
	Mean ± SD	N	Mean ± SD	N	Mean ± SD	N	Mean ± SD	N
1/4	0.050 ± 0.009	8	0.049 ± 0.002	3	0.037 ± 0.003 *	8	0.058 ± 0.022	8
2/1	0.451 ± 0.053	8	0.445 ± 0.052	3	0.288 ± 0.075 *	8	0.480 ± 0.058	8
4/1	0.726 ± 0.073	8	0.753 ± 0.098	3	0.603 ± 0.067 *	8	0.764 ± 0.070	8

725
726 * = $p<0.05$, Student's t-test with Bonferroni correction; N= number of slices
727
728
729 **Table 2:** Numbers of release sites and quantal amplitude estimated by variance/mean
730 analysis at Schaffer collateral synapses in field CA1

	CON/VEH		CON/7,8-DHF		Pb^{2+}/VEH		Pb^{2+}/7,8-DHF	
	Mean ± SD	N	Mean ± SD	N	Mean ± SD	N	Mean ± SD	N
N. Release	144 ± 57	8	108 ± 60	8	130 ± 53	8	126 ± 58	8
Quantal Amp	2.63 ± 0.48	8	2.56 ± 0.93	8	2.53 ± 0.58	8	2.43 ± 0.79	8

731
732 N= number of slices
733